ISSN 1027-5495. Functional Materials, 32, No.2 (2025), p. 277-291
doi:http://dx.doi.org/10.15407/fm32.02.277

Langmuir-Blodgett technology for creating electrochemiluminescent sensors

D. Martynov[1,2]***, E. Schlein***[3,4]***, M. Slipchenko***[1,3]***,***
D. Snizhko[2]***, Yu. Zholudov***[2]

[1]Institute for Scintillation Materials of the National Academy of Sciences of Ukraine, 60 Nauky Ave, 61072, Kharkiv, Ukraine
[2]Kharkiv National University of Radio Electronics, Department of Biomedical Engineering, 14 Nauky Ave, 61166, Kharkiv, Ukraine
[3]National Technical University «Kharkiv Polytechnic Institute», 2 Kyrpychova str., 61002, Kharkiv, Ukraine
[4]Leibniz Universität Hannover, Welfengarten 1, 30167 Hannover, Germany

Received May 2, 2025

This paper is devoted to the study of the properties of Langmuir-Blodgett films for electrochemiluminescence (ECL) analytical applications. Films of 9,10-diphenylanthracene (DPA) and rubrene in a matrix of polymeric and monomeric substances were investigated for surface wetting, photoluminescence, morphological, electrochemical and ECL characteristics. The results showed that the orientation of phosphor molecules in monomer and polymer films differs, which affects their wettability with water. According to the solid-phase fluorescence analysis, polymethyl methacrylate (PMMA) is a more effective transfer agent for DPA compared to stearic acid, since films based on it give a more intense fluorescence blue spectrum compared to the monomer. The atomic force microscopy (AFM) data show that polymethyl methacrylate forms periodic structures in the form of globules and plates, and the surface of the pure electrode is fine-grained with nanoscale structural elements. According to cyclic voltammetry, it can be seen that with an increase in the number of film layers, the electrochemical properties of the modified electrodes deteriorate, while the surface of different electrodes degrades equally. The ECL system based on film electrodes with tetraphenylborate co-reagent gives a noticeable ECL signal that is linear with the concentration of the co-reagent. Overall, the results emphasize the complex interplay between film structure, surface properties, and electrochemical performance, providing valuable information for the development of advanced sensor technologies.

Keywords: coreactant, electrochemiluminescence, Langmuir-Blodgett film, sensor

Технологія Ленгмюра-Блоджет для створення електрохемілюмінісцентних сенсорів. *Д. Мартинов, Є. Шлейн, М. Сліпченко, Д. Сніжко, Ю. Жолудов*

Стаття присвячена дослідженню властивостей плівок Ленгмюра-Блоджетт для електрохемілюмінесцентних (ЕХЛ) аналітичних застосувань. Плівки 9,10-дифенілантрацена (ДФА) та рубрена у матриці з полімерних і мономерних речовин було досліджено на поверхневе змочування, фотолюмінесцентні, морфологічні, електрохімічні і ЕХЛ характеристики. Результати показали, що орієнтація молекул люмінофорів в плівках мономерів та полімерів відрізняється, що впливає на їхню змочуванність водою. За даними твердофазного флуоресцентного аналізу поліметилметакрилат (ПММА) є більш ефективним переносним агентом для ДФА в порівнянні зі стеаринової кислотою, оскільки плівки на його основі дають більш інтенсивний сиграл флуоресценції в порівнянні з мономером. За даними атомно-силової мікроскопії (АСМ) видно, що поліметилметакрилат утворює періодичні структури у вигляді глобул і пластин, а поверхня чистого електроду дрібнозерниста з нанорозмірними структурними елементами. За даними циклічної вольтамперометрії видно, що зі збільшенням кількості шарів плівки електрохімічні властивості модифікованих електродів гіршають, при цьому поверхня різних електродів деградує однаково. ЕХЛ система на основі плівкових електродів зі співреагентом тетрафенілборатом дає помітний ЕХЛ–сигнал, лінійний від концентрації співреагенту. Загалом, результати підкреслюють складну взаємодію між структурою плівки, властивостями поверхні та електрохімічними характеристиками, надаючи цінну інформацію для розробки передових сенсорних технологій.

1. Introduction

The modern development of science is accompanied by new challenges, in particular in analytical chemistry, where it is necessary to improve analysis methods or develop new approaches. Of particular importance is the study of biological and environmental objects that may pose a threat to human health and ecosystems. One of the most promising analytical methods is electrogenerated chemiluminescence (ECL). Since the 1960s, researchers, including those led by Allen Bard and David Hercules, have been studying ECL, although the first mention of this phenomenon dates back to the 1920s. The method attracted considerable attention in the 1980s, after the creation of efficient ECL systems based on tris(bipyridine)rut henium(II). Since then, ECL research has been actively developing, and this method, which is superior to traditional optical luminescence in terms of sensitivity and flexibility, has become an important research and analysis tool [1].

The method is important due to its ability to detect analytes in immunological analysis and its applicability in biology, medicine, ecology, food industry and pharmacology due to its ability to detect nitrogen-containing compounds that are part of DNA, RNA, amino acids, proteins, neurotransmitters and a number of other biologically significant substances [2].

ECL is a non-thermal emission of light resulting from the transfer of electrons at the electrode surface, inducing a cascade of chemical reactions that lead to the formation of a photon with a characteristic wavelength, which is an analytical signal [3].

This phenomenon combines electrochemical and chemiluminescent (CL) natures: photon emission occurs during electron density relaxation, and electron excitation occurs during electron transfer between particles formed during electrolysis. As an example, in the recombination scheme of ECL, which is mostly implemented in aprotic solvents, electron acceptors are reduced at the cathode to form anion radicals, and donors are oxidized at the anode to form cation radicals. Ion radicals interact in the reaction zone near the electrode via mass transfer to form an activated phosphor complex, which decays with the emission of light [4]. The light intensity is proportional to the number of phosphor species, and the resulting light flux is recorded by a photodetector or spectrometer [5], while ECL allows recording voltammograms and voltlumenograms, which allow studying electrochemical transformations and kinetics of processes at the electrodes. Due to the absence of a background excitation signal and the ability to generate reagents *in situ*, ECL provides high sensitivity and signal linearity over several orders of magnitude [6]. ECL, as a subsection of chemiluminescence (CL) and electrochemistry, retains their advantages while eliminating their main drawbacks.

Firstly, the temporal and spatial control of ECL electrochemical steps allows for delayed luminescence during immune or enzymatic reactions, reducing background emission and improving detection sensitivity [7]. The spatially distributed positions of detectors and reaction sites in ECL cells allow for multiple reactions to be performed simultaneously, for example, using magnetic spheres to distinguish between bound and unbound labels [8], or at the arrays of electrodes with programmable activation [9]. Secondly, ECL is highly selective due to the dependence of the redox processes of participating particles on the applied electrode potential [10]. And thirdly, the phosphor species in ECL can be recycled and reused for signaling, i.e. ECL is a non-destructive method [11]. Unlike photoluminescence, ECL does not involve a light source, eliminating problems with stray light and luminescent impurities. The specificity of ECL reactions with the coreactant reduces side effects such as self-quenching and provides high signal-to-noise ratio and compatibility with various detector platforms [12-13].

There are more than 150 enzyme-linked immunosorbent assays on the market for various conditions, from heart disease to tumor marker detection, from the leaders in this field, Roche Diagnostics Inc. and Meso Scale Discovery Inc

[14]. ECL assays are widely used in medical diagnostics to detect even small amounts of specific antibodies in blood or urine samples, and to diagnose various pathologies, including cardiac or infectious diseases, thyroid dysfunction, and tumor markers [15]. Some well-known phosphors, such as 9,10-diphenylanthracene, are used in ECL assays to analyse aflatoxin B1 produced by *Aspergillus parasiticus* [16], as well as to determine microRNA-141, a biomarker of prostate cancer [17]. ECL has a significant potential in the analysis of biological and environmental samples. It can be used both as an independent method for analyzing complex systems with different substances and matrices, and as an auxiliary detection tool in related analysis methods. This raises the challenge of developing and optimising new analytical devices to improve the accuracy of the analysis results. The development of highly sensitive ECL sensors is one of the ways to solve this problem.

Aqueous media are important for chemical analysis, requiring the search for water-soluble phosphors and coreactants. However, these media have a limited range of available electrode potentials, and free protons affect the formation and stability of radical ions. It also requires to use relatively large amounts of phosphor in solution [1]. Electrodes modified with insoluble phosphors or their compositions solve these problems by allowing the use of tiny amount of phosphor in the film. ECL sensors – electrodes with an inert organic film incorporating phosphor species – play an important role in modern chemical analytics. They enable measurements in aqueous media using insoluble phosphors, reducing costs and improving process control [18].

There are numerous methods of film deposition, each of which affects the thickness, uniformity, composition and adhesion to the substrate. The main methods are centrifugation, dipping, physical or chemical vapour deposition, atomic layer deposition, electrodeposition, sol-gel, thermal vacuum sputtering, molecular beam epitaxy, as well as promising techniques such as self-assembled monolayers and guest-host technology [19]. All methods have their advantages (speed, wide range of materials, control of homogeneity and temperature) and disadvantages (difficulty in controlling viscosity, number of layers and molecules, microarchitecture and morphology stability).

The Langmuir-Blodgett (LB) method allows the creation of monomolecular films with a high level of order, which allows for precise control of their composition, structure and thickness. This makes LB films promising for the development of molecular systems for ECL excitation. LB technology allows to adjust the surface density of molecules and intermolecular distances between luminescent centres, which affects the non-radiative energy transfer within the film (Förster and Dexter mechanisms), important for efficient ECL emission. In addition, the LB electrode modification technology allows us to study the effect of the number of layers on sensor performance and physical and chemical processes on the electrode surface. [20]

LB technology allows the creation of monolayers of insoluble substances at the solvent-air interface (usually on the surface of water). Functional molecules or nanoparticles are incorporated into amphiphilic transfer agents, such as fatty acids or polymers, to form a stable monolayer that can be fixed on the surface of water or transferred to a substrate (like an electrode) [21]. There are two main transfer methods: vertical (Langmuir-Blodgett) and horizontal immersion (Langmuir-Schaefer). The immersion rate controls the amount of molecules adsorbed, and the barrier maintains a uniform surface pressure. The molecules can be orientated in three possible ways: X – the hydrophobic part towards the substrate surface, Y – the orientation of the hydrophilic/hydrophobic parts alternates in each film layer, Z – the hydrophilic part towards the substrate surface. Y-type films are the most stable due to the optimal relative orientation of the hydrophobic and hydrophilic parts of the molecules in the film. The LB technology allows for precise adjustment of film parameters (molecular orientation, density, thickness), which makes it promising for research purposes. The combination of LB with ECL opens up opportunities for optimising film parameters to analyse and investigate reaction mechanisms on the electrode surface, as well as to study physicochemical processes during the electrolysis of the phosphor-solvent system in heterogeneous ECL reactions.

2. Experimental

LB films with different phosphors and matrix substances were used in the work: polymethyl methacrylate (PMMA) and stearic acid (HSt) as matrices, 9,10-diphenylanthracene (DPA) and rubrene (Rub) as phosphors. The films were deposited using an LB trough LT-103 (Microtestmachines Co) on transpar-

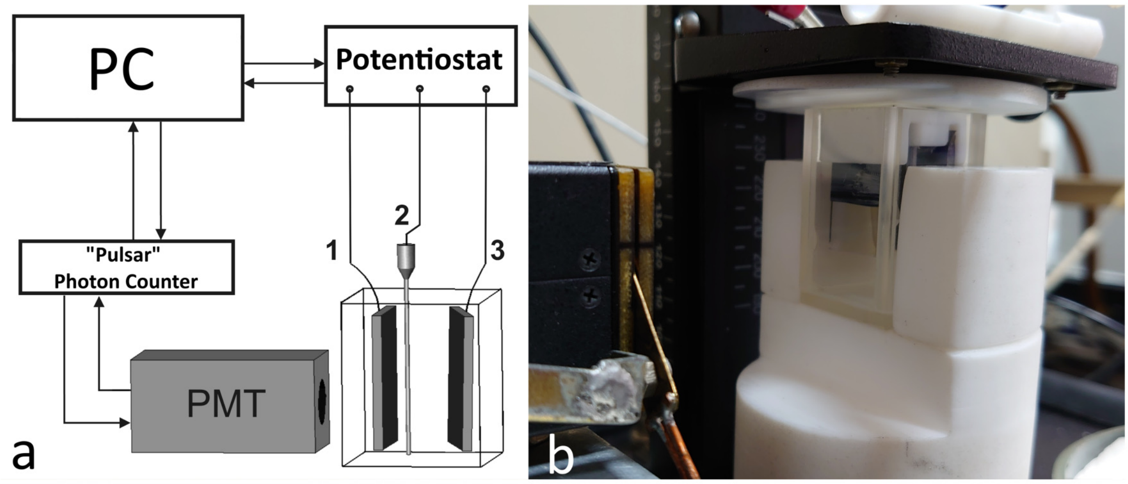

Fig. 1. Schematic of the experimental setup: 1 – working electrode, 2 – reference electrode, 3 – auxiliary electrode (a), and photograph of the ECL cuvette module (b)

ent ITO electrodes (25× 15 mm). The surface morphology was studied using an atomic force microscope (AFM) NT-206 (Microtestmachines Co). Spectroscopic measurements were performed using an OceanOptics QE65000 spectrometer with a laser excitation source LSR405NL (λ = 405 nm). Mathematical processing of the spectral data was performed using the SpectraSuite software.

Electrochemical and ECL studies were carried out by cyclic voltammetry technique (100 mV/s potential sweep rate) in phosphate buffer (0.2 M) prepared using double distilled water. The ECL coreactants were tripropylamine (TPrA) and sodium tetraphenylborate (TPhBN). The solutions were bubbled for 10 minutes before experiments (in case of TPrA coreactant – before its addition, since TPrA is volatile). The experiments were carried out in the cuvette module of ELAN-3D ECL analyser [22] using an Autolab PGSTAT128N potentiostat, photon counting PMT module H10682-210, and Pulsar photon counter [23]. The ECL compositions were placed in a rectangular quartz cuvette with the working ITO electrode, silver chloride the reference electrode in the form of a syringe, and a glass carbon plate auxiliary electrode (Fig. 1) [22]. During ECL studies, dissolved oxygen was removed from the solution by bubbling with argon through a polyethylene capillary.

2.1 Preparation of solutions

The selection of solution concentrations for films deposition was based on the results of O.N. Bezkrovnaya and co-authors [24]. To prepare the solutions, we used separate weights of polymer and phosphor in Eppendorf plastic tubes, which allows us to standardise the concentration of components and speed up the dissolution. To do this, a solution of the required concentration was made in a volatile solvent and spread over the plastic tubes until they dried. These tubes with film components became standard titres. 9,10-diphenylanthracene is photo stable, while rubrene is not and can lose its luminescent properties when phototreated, so rubrene solutions were prepared before each deposition cycle. The detailed process of preparing solutions is described in our previous paper [25] and the patent [26].

To study the linearity of the ECL intensity with the concentration of the coreactant, standard solutions of Ph_4BNa of different concentrations were prepared: $1 \cdot 10^{-6}$, $1 \cdot 10^{-5}$, $1 \cdot 10^{-4}$, $1 \cdot 10^{-3}$ M. For this purpose, 2.0 ml of Ph_4BNa stock solution (0.01 M) was prepared and diluted with phosphate buffer solution to obtain the required working solution concentrations.

2.2 Langmuir-Blodgett films deposition parameters

The basic parameters for the deposition of Langmuir-Blodgett films were taken from [24]. The working solution is added in 50 μl portions, which are evenly distributed in droplets over the bath surface, with breaks for film relaxation, until the film pressure reaches 15 mN/m. The film is then compressed to the working pressure (25 mN/m) by a barrier moving at a speed of 0.3 mm/s in 5 mm increments. The immersion speed of the substrate is set depending on the film type (0.020 mm/s or 1.200 mm/s), and the immersion depth is 20 mm. The operating pressure is selected from the film compression isotherms as the midpoint

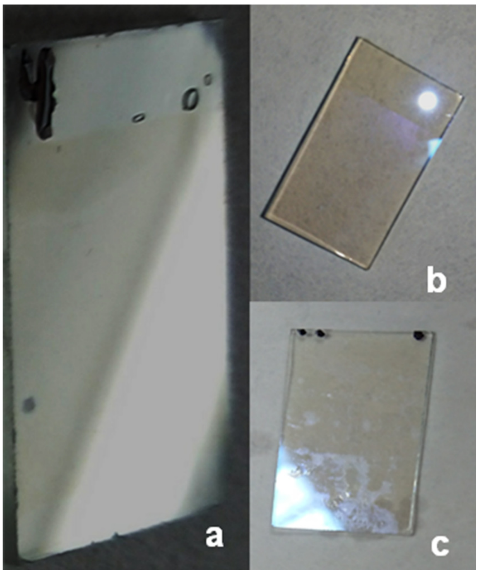

Fig. 2. Photographs of the obtained modified electrodes: a and b – after film deposition; c – after electrolysis.

of the curve corresponding to the solid phase of the film on the surface (for HSt and PMMA, it is 25 mN/m). Fig.2 shows examples of the obtained modified electrodes.

Preliminary ECL studies have shown that cleaning of used electrodes by soaking in chloroform is not sufficient, so a vapor degreasing system based on a Soxhlet extractor with a copper coil condenser was made for better cleaning. Electrode cleaning in this system is cyclical: washing with condensed vapours, soaking in the accumulated distillate and draining the washing solution. The cleaning was performed in 5 cycles.

3 Results and discussion

To understand the quality and structure of the film, a number of studies were carried out: surface wetting and evaluation of hydrophilicity and hydrophobicity of the films by the sessile drop method, photoluminescent properties by solid-state fluorometry, surface morphology by atomic force microscopy, electrochemical properties by cyclic voltammetry and ECL studies.

3.1 Wettability and contact angle measurements

The wettability of the sensors' surface was studied using the sessile drop method, which allows us to estimate the orientation of molecules based on changes in hydrophilicity or hydrophobicity (Fig. 3). When films are deposited by the LB method, amphiphilic molecules are oriented in such a way that X- and Z-type films should be hydrophilic and hydrophobic, respectively. An increase in the contact angle indicates hydrophobicity, and a decrease in the contact angle indicates hydrophilicity. A 10 µl drop of water was placed on the electrode surface, photographed at different angles, and the wetting angle was estimated using a custom-made software (Fig. 3e). This analysis allows us to judge the orientation of the molecules on the surface at the statistical level. It is known from previous work, based on the analysis of Langmuir compression isotherms of films, that the arrangement of phosphor molecules differs in HSt and PMMA LB matrices [24]. In the PMMA/rubrene system, the main plane of rubrene molecule is partially shifted to the monomolecular layer: the benzene rings are in-

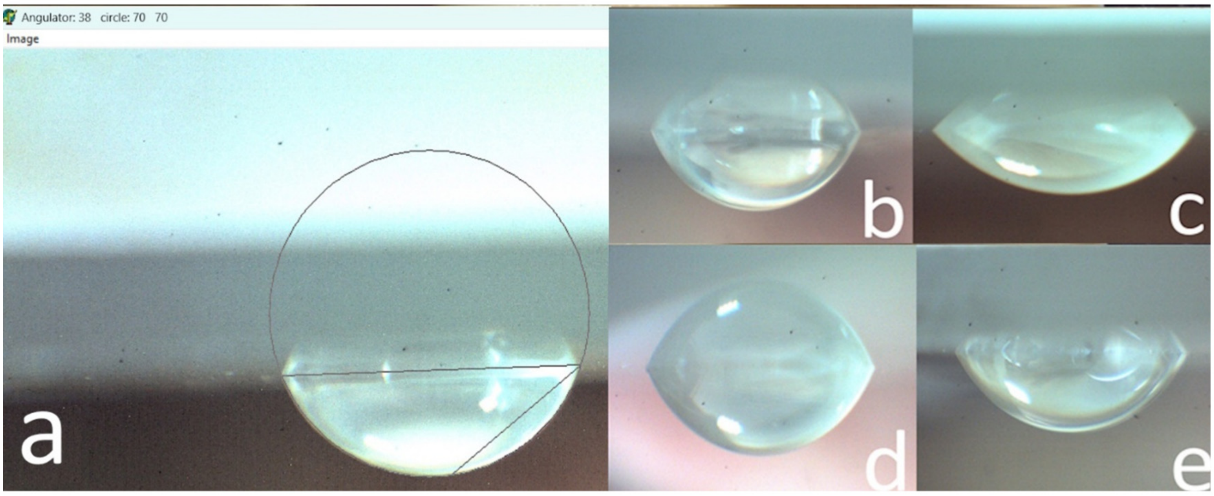

Fig. 3. The calculations were performed using custom-made software (a). Examples of measuring the contact angle of ITO electrodes with different films: Z-type PMMA film - 54° (b), X-type PMMA film - 45° (c), Z-type - 55° (d), X-type HSt film - 50° (e).

Table 1. Changes in the contact angle for single-layer films of matrix substance (without phosphor) of different types of application.

Substance	Edge wetting angle	Clean electrode	Film		Average difference
			Z-type	X-type	
PMMA film	ITO layer	66,0°	54,0°	-	-12,0°
HSt film	ITO layer	48,0°	-	42,0°	-6,0°

Table 2. Variation of the contact angle for stearic acid films (without phosphor) of different types of application.

Contact angle	Clean electrode	Film			Average difference
		Z-type	X-type	ZY-type	
ITO layer	52,5°	54,5°	-	-	+2,0°
	67,0°	-	57,0°	-	-10,0°
	52,5°	-	-	83,0°	+30,5°

side, and the rest of the molecule is pushed to the surface due to hydrophobic properties. At the same time, a change in the conformation of rubrene molecules is observed, in particular, a «plateau» is detected in the compression isotherms, which is associated with the transformation of molecules in the monomolecular layer, and the luminescence spectrum experiences hypsochromic shift. In the HSt/rubrene system, the basic plane of the phosphor molecule is located between the alkyl chains, and with increasing phosphor concentration, the molecules aggregate and separate phases are formed (according to [27], with increasing pressure, better ordering occurs, so there is a problem of the collapse limit). Since the rubrene molecule is similar to the DPA molecule, the orientation and arrangement of molecules in rubrene and DPA systems are expected to be similar.

Table 1 shows the variation of the contact angle for single-layer films of matrix substance only with different orientations. For the HSt films, the angle decreases for the X-type, indicating an increase in hydrophilicity, which is consistent with theory. In contrast, no such effect was observed for PMMA. The Z-type film also reduces the contact angle, although it should be hydrophobic according to theory. It is worth noting that for the back glass side of the electrode, the angle increases for all film types, probably due to excellent adhesion to glass. Since HSt is a monomeric substance, the theoretical and practical change in wetting should coincide for its films. Table 2 confirms this: for X-type films, the angle decreases (more hydrophilic), for Z-type films, it increases (more hydrophobic), and for ZY films, the change is almost 31°, which is explained by the three-layer structure. The glass side shows a similar trend.

Table 3 shows contact angles for PMMA films with incorporated DPA phosphor on chemically modified electrodes after several electrolysis cycles. The results from Table 3 are in line with theoretical expectations: for Y- and Z-type films, the wetting angle is larger (hydrophobic), and for X-type films, it is smaller (hydrophilic compared to Y-type films). Table 4 shows the data for a new electrode surface that was not in use. Here again, for the conductive ITO surface, the change in the contact angle does not meet the theoretical expectations, while the opposite trend is observed for the glass side of the electrode. It can be assumed that the fresh electrodes have different structural properties and the number of active centres for adsorption, which affects the adhesion of the polymeric substance. Polymers have a complex spatial structure, so both in solution and in Langmuir-Blodgett films, additional surface relaxation can be expected over time, when polymer tangles with trapped phosphor molecules occupy the most thermodynamically favourable conformation and orientation of individual substituents in space relative to the electrode surface itself and adjacent neighbouring layers. For monomeric substances, such changes are less pronounced.

The sessile drop method is quite fast and versatile for assessing surface changes during modification, but is not very useful for studying the local microstructure of the film. However, the method proved that the expected change in wettability corresponds to the type of film application used, with the first layers showing a smaller change in the contact angle of the monomer film than similar polymer films, while the second and third layers for monomer films change the angle more than for similar

Table 3. Changes in the contact angle for PMMA/DPA films of different types of deposition on electrodes with degraded (electrolysed) surfaces.

Contact angle	Clean electrode	Film		
		Z-type	Y-type	YX-type
ITO layer	45,9±0,9°	68,7±1,1°	66,6±1,1°	55,3±1,1°
The difference is relatively...		Z-type	Y-type	YX-type
ITO layer	Clean electrode	+23,0°	+21,0°	+9,4°
ITO layer	Y-type	-	-	-11,3°

Table 4. Changes in the contact angle for PMMA/DPA films of different types of deposition on electrodes with a new (not electrolysed) surface.

Contact angle	Electrode	Clean electrode	Cleaning with chloroform	The difference	Film		
					Z-type	Y-type	YX-type
ITO layer	1	90,3±1,4°	82,3±0,5°	-8,0°	72,5±0,6°	-	-
	2	89,4±1,0°	76,1±0,5°	-13,3°	-	74,4±0,6°	-
	3	97,7±0,9°	75,7±0,9°	-22°	-	-	91,8±0,5°
	4	94,3±0,5°	82,8±0,8°	-11,5°	-	-	-
The difference					-9,8°	-1,7°	+16,1°

polymer films (for HSt, single-layer films change the angle by 1° - 10°, while for PMMA it is 10° - 20°, and for three-layer films, the ranges are reversed).

3.2 Fluorescent properties of films

The photoluminescence properties of the prepared sensors were investigated by solid-phase fluorometry. In this work, polycyclic aromatic hydrocarbon DPA with 3 benzene rings in the skeleton was studied, which belong to conjugated systems with an electron cloud of π-electrons, providing its capability for photoluminescence. The characteristics of the luminescence spectrum and intensity can be used to estimate the presence of phosphor molecules, its solvatochrome properties, and concentration, which is proportional to signal intensity. The use of optically transparent ITO electrodes prevents the luminescence signal from being quenched by the electrode material, simplifying the analysis. A semiconductor laser with a wavelength of 405 nm was used for fluorescence excitation. To minimise photobleaching of phosphor molecules, the study was carried out in a pulsed mode with the signal recorded through a glass filter ЖС-11 to cut off scattered excitation signal (cuts off the UV range, transmittance less than 10% for wavelengths shorter than 410 nm).

Fig. 4 shows the luminescence spectra of HSt/DPA films of different types and thicknesses. The double-layer Y film has a higher intensity than the single-layer Z and X types, with the Z type showing a slightly higher intensity. This can be attributed to different orientation of hydrophobic tails of HSt, where the phosphor molecules are concentrated, and thus different proximity of phosphor molecules to electrode surface/ambient air causing different level of possible quenching and non-radiative relaxation processes.

Fig. 5 shows the luminescence spectra of HSt/DPA (2, 4, and 6 layers) and PMMA/DPA (1, 2, and 4 layers) films, as well as the peak intensity values for each sensor type. The figure shows that the shape of the luminescence spectrum differs significantly, with the luminescence intensity for the polymer matrix being higher than that of the monomer matrix (for 2 and 4 layers), the difference for 2-layer films almost reaching 1.8 times. The shape of the intensity vs. layers curve suggests that polymer films are subject to a certain luminescence limit, while monomer films are not. At the same time for thinner films fluorescence is more efficient in PMMD/DPA systems thus assuming requirements for electrochemical experiments (an increase in the number of layers leads to a decrease in the electrochemical activity of the

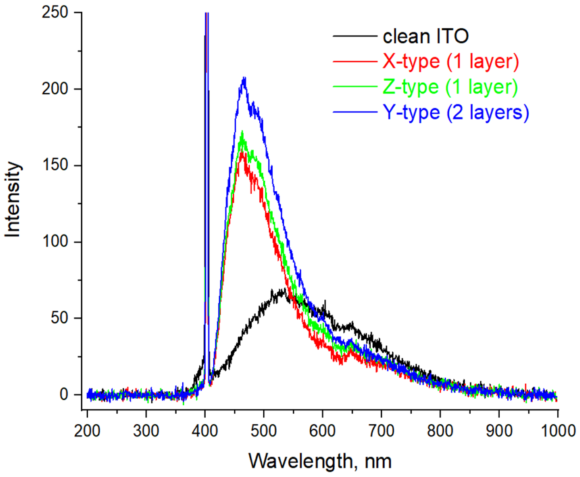

Fig. 4. Luminescence spectra of HSt/DPA films: pure electrode (black), single-layer X-type film (red), single-layer Z-type film (green), double-layer Y-type film (blue).

surface, see part 3.4), the PMMA matrix should give more advantages.

Our studies of Rub films have shown significant differences in the spectra compared to DPA (similar HSt films, 4 layers, YY-type). The spectral peak for Rub is batochromically shifted and has a lower intensity. As noted, rubrene is not photostable and degrades even in the pulsed mode, although its stability to electrolysis is known to be higher than that of DPA. DPA is also susceptible to degradation during ECL analysis, but photodegradation of Rub during sensors fabrication completely eliminates the possibility of obtaining reproducible ECL signals. Therefore, the paper presents the results of studies only with DPA as a more stable phosphor. The studies have shown the time-dependent photoluminescent properties of the films: exposure of the films in the dark causes an increase in the optical signal. This effect persists for both DPA and Rub, and more pronounced for Rub. This can be explained by the relaxation of the film structure. Since it is quite thin, the degrees of freedom for it are greater than for molecules in thick films, at least due to the greater amount of Gibbs free energy, which is a well-known fact in nanoscience [28]. These studies have shown that the polymer is a better transfer agent for phosphors compared to HSt. The relaxation of the film increases the light emission signal, with DPA giving a higher signal and being more photostable, so it was used in further studies. For the PMMA matrix, a batochromic shift in the luminescence spectrum is observed with an increase in the number of layers, which does not occur for HSt. This can be explained by the difference in the distribution of phosphors in the films and, accordingly, different conditions for the interaction between phosphor molecules in adjacent layers. The fact that the matrix affects the formation of the energy levels of the excited states of phosphors is known from the literature [24].

3.3 Film morphology

The surface morphology of the obtained sensors based on PMMA/DPA films was studied by atomic force microscopy. Fig. 6a shows an AFM image of the surface of a pure electrode without a film (2.1 μm × 1.9 μm area), which shows the fine-grained structure of tin-indium oxides themselves, fractal dimension 2.72. Fig. 6b shows an AFM image of the sensor surface with a two-layer PMMA/DPA Y-type film (2.5 μm × 2.5 μm), which demonstrates the formation of globules and plates with a fractal dimension of 2.82.

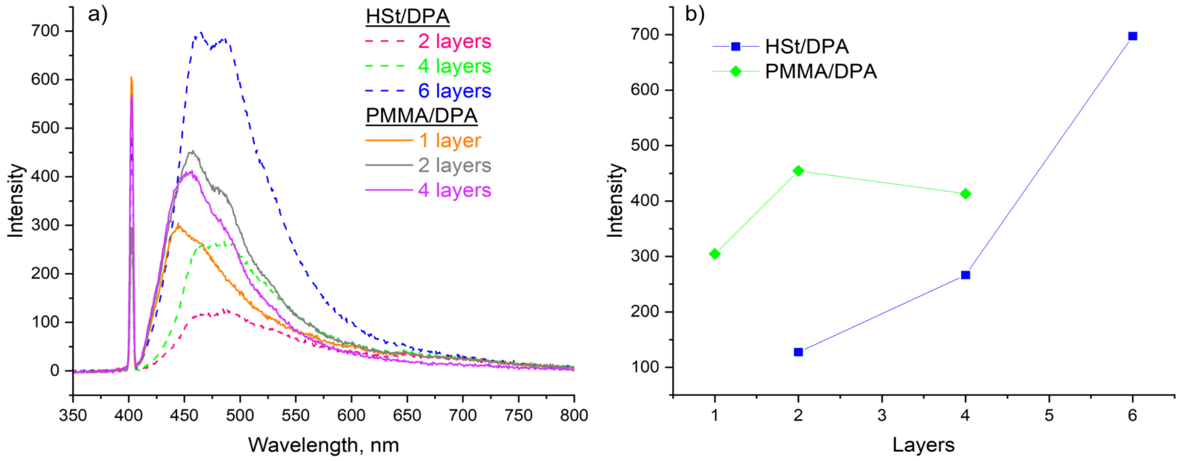

Fig. 5. Dependence of the luminescence intensity of HSt/DPA (2, 4 and 6 layers) and PMMA/DPA (1, 2 and 4 layers) films on the number of layers and matrix substance (left), as well as the dependence of the maximum intensity for films of different composition on the number of layers (right).

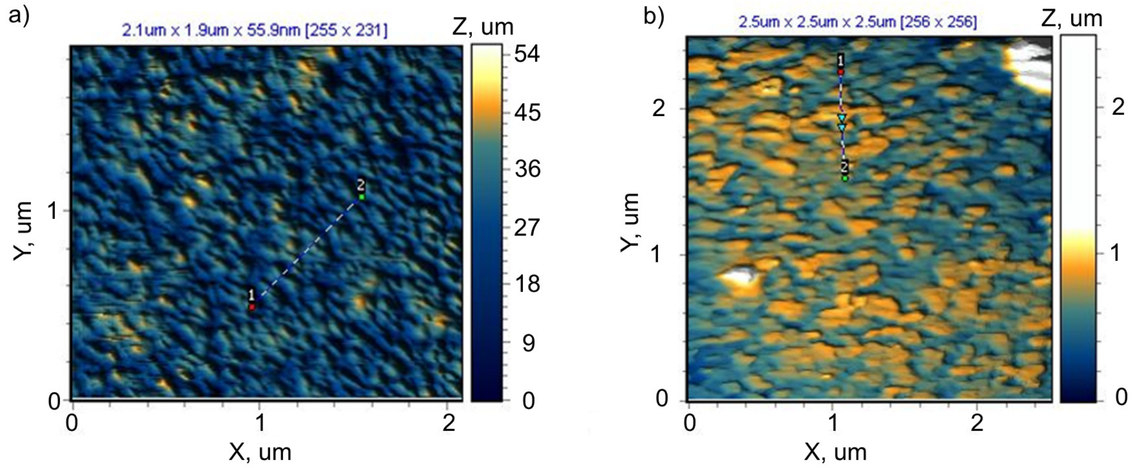

Fig. 6. AFM images of the pure ITO electrode surface (a) and the electrode modified with 2 layers of PMMA/DPA Y-type film (b)

This indicates a dense coating of the electrode. The change in the fractal dimension indicates the branching of the structure and the increasing heterogeneity of the surface.

An important practical aspect for creating ECL sensors with LB films is the applicability of used ITO substrates after previous electrochemical experiments (degraded electrodes). Fig. 7 shows comparison of surface morphology of new and degraded electrodes in without films and with films of different structure. The degraded electrode without the film shows a fine-grained surface with grains up to nanometres high, while the new electrode without the film is characterised by a surface consisting of blurred structures up to 0.5 μm in size and 5-25 nm high.

For a Z-type film (single-layer) on a degraded electrode, the surface roughness indicators show the development of a granular structure with well-defined peaks, which is much more developed than the substrate itself. For the same film on the surface of a new electrode, structures similar to the pure substrate are observed, but the height profile is reduced by half and approaches that of the film on the degraded ITO substrate.

For the Y-type film (two-layer), a well-defined grain structure with grain sizes of 0.2 μm and a height of up to 10-15 nm is observed on the degraded electrode. On the surface of the new electrode, substrate structures are visible, but much less pronounced and smoothed.

For the XY-type film (three-layer) on the degraded electrode, the graininess is less pronounced compared to the two-layer film, but with a grain height 1.5 times larger. Single inclusions with a height of 50-70 nm and sizes up to 1.0 μm are found on the surface of the new electrode.

Thus, significant differences in surface morphology are observed between new and used electrodes, which confirms the slow degradation of the surface during operation and coincides with similar results from the literature [29]. The application of the film changes the surface topology, with the surface becoming more granular on degraded electrodes and more homogeneous on new electrodes. The most thermodynamically stable Y-type films show high grain size, which indicates effective transfer, especially on degraded electrodes, where such a film forms a rough surface.

3.4 Electrochemical properties of electrodes

The electrochemical properties of the obtained sensors were studied by cyclic voltammetry technique. We conducted separate studies of the redox couple Fe^{2+}/Fe^{3+} in a millimolar solution of iron (II) and (III) hexacyanoferrates in a phosphate buffer (pH ~ 6.8), scan rate 20 mV/s. Both pure electrodes with degraded and new surfaces, with PMMA and PMMA/DPA films were studied. Fig. 8a compares partially degraded electrodes with new ones. The degraded electrodes have lower electrochemical activity, which is manifested in broadened peaks of redox reactions of lower amplitude. The anodic peak for them is in the range of 0.5-0.8 V, with amplitude of 0.12-0.16 mA, exhibiting similar electrochemical properties and homogeneous surface degradation regardless of the number of electrolysis cycles. Compared to them, the new electrodes have well defined anode and cathode current peaks, with a narrower potential shift between them and higher amplitudes. These results correlate with the

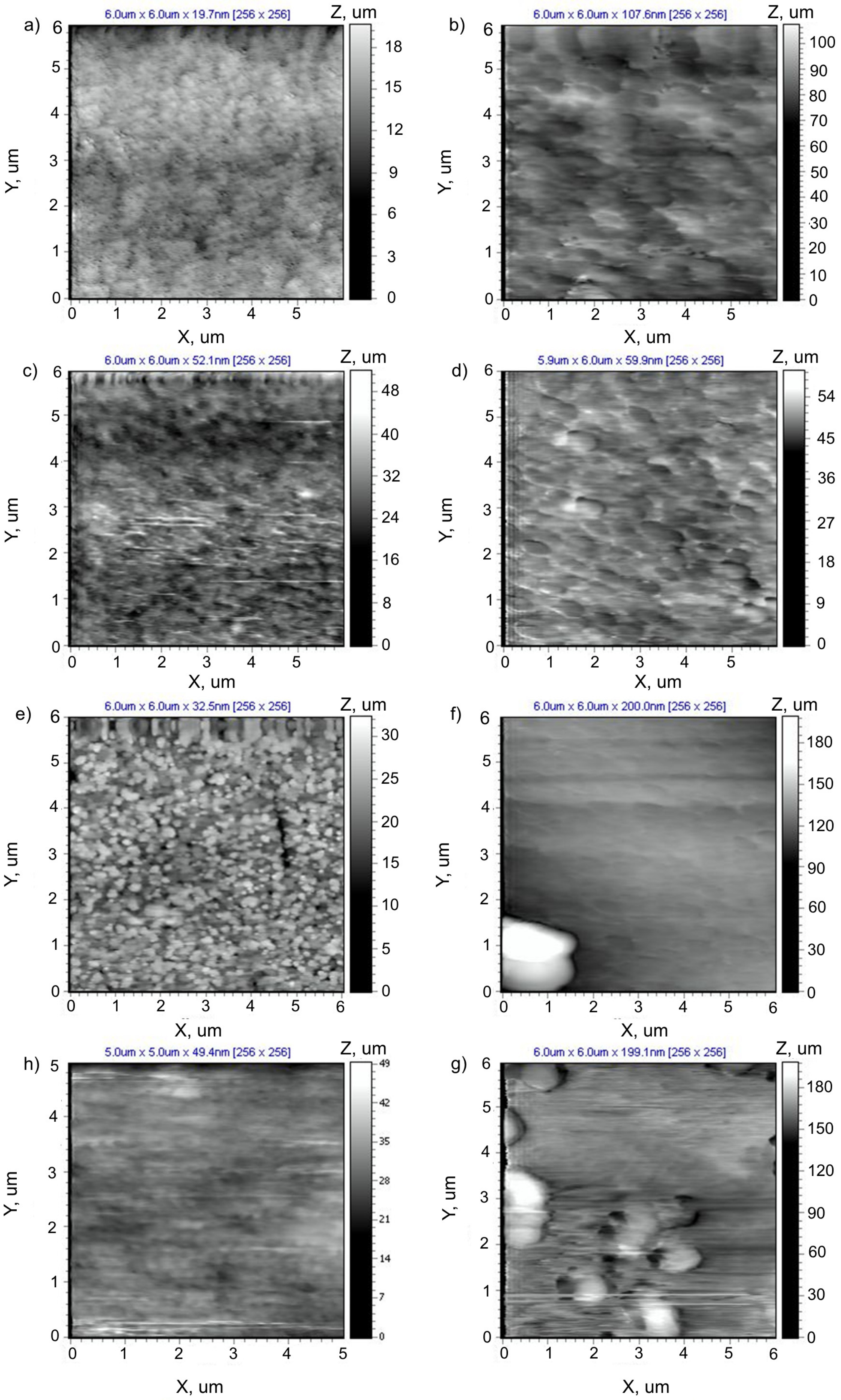

Fig. 7. AFM images of the electrodes: clean degraded (a) and new (b) electrodes; Z-film of PMMA/DPA on degraded (c) and new (d) electrodes; Y-film of PMMA/DPA on degraded (e) and new (f) electrodes; XY-film of PMMA/DPA on degraded (g) and new (h) electrodes.

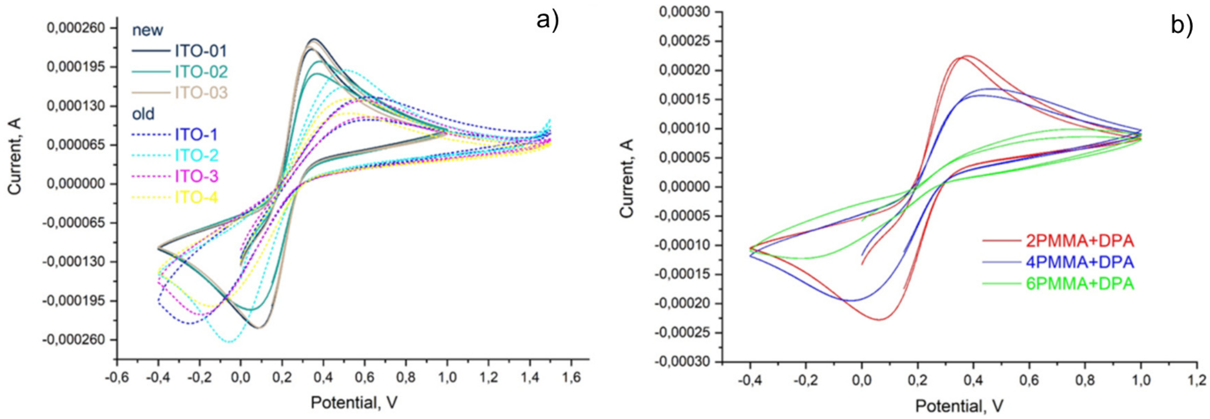

Fig. 8. Voltammograms of ITO electrodes in Fe^{2+}/Fe^{3+} solution (1 mM) in phosphate buffer. (a) Clean electrodes with degraded and new surfaces. (b) New ITO electrodes with PMMA/DPA Y-type films of 2, 4 and 6 layers thickness.

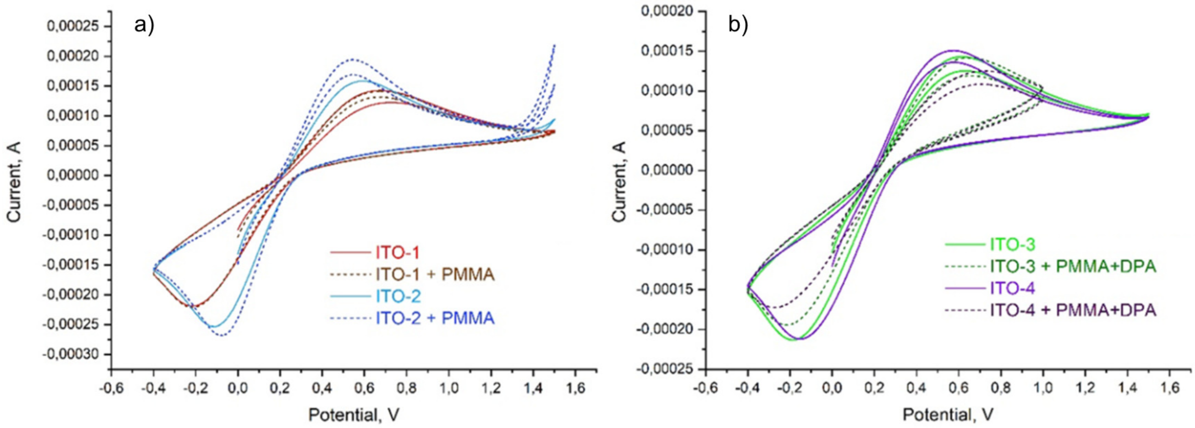

Fig. 9. Voltammograms of ITO electrodes with partially degraded surface in Fe^{2+}/Fe^{3+}) solution (1 mM) in phosphate buffer. Comparison of pure electrodes and electrodes with a double-layer film (a) PMMA Y-type, (b) PMMA/DPA Y-type.

AFM studies, showing that after electrolysis ITO electrodes degrade and their surface becomes smoother.

Fig. 8b shows the results of studying the electrochemical activity of new electrodes with different number of PMMA/DPA layers. An increase in film thickness (from 2 to 6 layers) leads to increased surface passivation. According to [20], the optimal range is 1-6 layers of LB, with a decrease in ECL (Schaefer deposition technique) above that number. For the Langmuir-Blodgett method, 2 layers of film are optimal according to the electrochemical behaviour.

The availability of the electrode surface for electron transfer is critical for electrochemical processes. Fig. 9a shows the voltammetry for the degraded electrodes before and after the application of a two-layer film of pure Y-type PMMA matrix. The change in the electrochemical properties of the modified electrodes is not significant, whereas in some cases (ITO-2) the electrochemical activity after the PMMA film application has improved to some extent, which is a rather unexpected result. Fig. 9b shows the voltammograms for the electrodes before and after the application of a two-layer PMMA/DPA Y-type film. After the film is applied, a decrease in electrochemical activity is observed, especially in the cathode region, indicating a decrease in the availability of the electrode surface for redox processes. However, the changes are not significant, and the nature of the electrochemical behaviour of the surface remains almost unchanged, showing only a slight passivation.

The results indicate that the reused electrodes are fully suitable for the manufacture of sensors. The films with phosphor further reduce the electrochemical activity comparing to pure PMMA films, which may be the result of blocking the existing pores between the polymer globules by DPA molecules thus limiting the accessibility of the electrode surface. The most significant factor affecting electrochemical

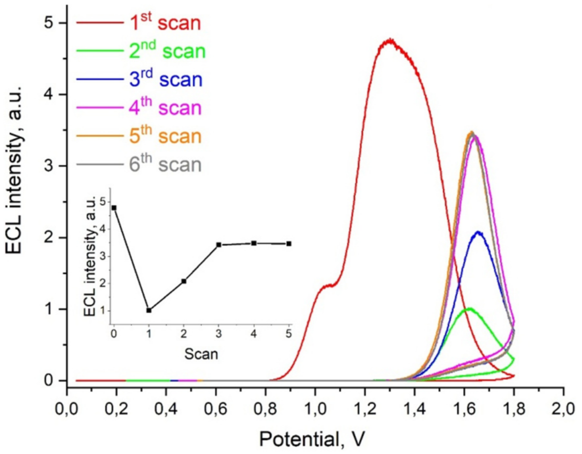

Fig. 10. ECL response for a PMMA/DPA Y-type bilayer film. Coreactant 0.6 mM Ph_4BNa in phosphate buffer (0.2 M), scanning speed 100 mV/s. Inset: dependence of the ECL peak maximum on the scan cycle number.

activity is the number of film layers. Increasing the film thickness reduces the availability of the analyte for reactions with the electrode. Thus, when selecting the film thickness, it is important to consider the balance between its stability and electrochemical activity to achieve optimal sensor sensitivity.

3.5 Electrochemiluminescence studies

ECL studies were carried out in phosphate buffer with the addition of Ph_4BNa as a coreactant by cyclic voltammetry at a potential scanning rate of 100 mV/s. Fig. 10 shows the ECL response of a sensor based on Y-type bilayer a PMMA/DPA film for a sequence of potential scanning cycles. During 1^{st} cycle two clearly separated ECL waves are observed, corresponding to redox reactions: the first peak is at 1.05 V, the second is at 1.30 V. The shape of the ECL curve changes from scan to scan: after the first scan, which gives a two-peak ECL, subsequent scans show an ECL signal that shifts to higher potentials, drops in intensity and tends to further growth with each electrolysis cycle, then reaches a certain maximum and then slowly decreases. These ECL curves have the character of narrow peaks and are located in the region of water decomposition potentials. This can be explained by the fact that after the first cycle, oxidation products of Ph_4BNa – biphenyl and its polymerisation products – are formed on the electrode, which can exhibit self-luminescence and sensitise the phosphor in the film [30]. These products are adsorbed on the electrode surface and prevent further redox reactions on the electrode, reduce the electrolysis current and lead to a potential shift in the observed responses.

The excitation of the phosphor in the film and the accessibility of the electrode largely depend on the permeability of the film and its structure, as well as the state of the electrode surface. The shape of the ECL response depends on the state of the electrode surface and the film structure. Fig. 11 shows the ECL signals and voltammetry for single-layer Z-type, two-layer Y-type, three-layer YX-type, and eight-layer Y-type PMMA/DPA films in reaction with Ph_4BNa. The voltammograms demonstrate an oxidation peak that shifts to lower potentials with increasing number of layers and disappears for eight-layer films. The ECL waveforms also vary with the number of film layers. For a single-layer film, the peak is shifted to lower

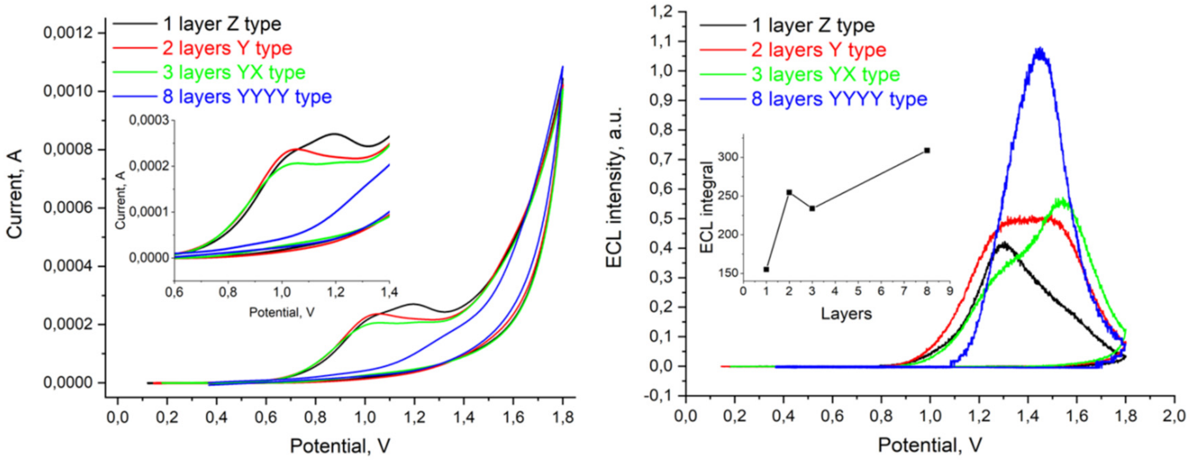

Fig. 11: Voltammogram (a) and ECL response (b) for sensors based on 1-layer Z-type, 2-layer Y-type, 3-layer XY-type, 8-layer 4Y-type PMMA/DPA films. Coreactant 0.67 mM Ph_4BNa in phosphate buffer (0.2 M), scanning speed 100 mV/s.

Table 5. Calibration equations for electrodes with different number of applied LB film layers.

Number of Layers	Type Films	Equation $pI = a + c\,pC$	R^2
1	Z	$(0.40\pm0.04)pC$	0,982
2	Y	$-(1{,}61\pm0{,}12)+(0{,}41\pm0{,}03)pC$	0,992
3	YX	$-(1{,}72\pm0{,}11)+(0{,}42\pm0{,}02)pC$	0,993

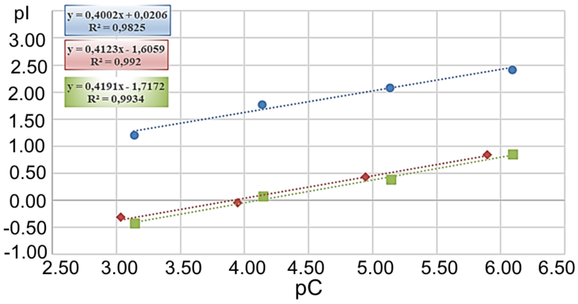

Fig. 12. Calibration plots of the dependence of the ECL intensity for sensors based on PMMA/DPA films on the concentration of Ph_4BNa films: single-layer Z-type (blue, circles), double-layer Y-type (red, diamonds) and triple-layer XY-type (green, squares). Phosphate buffer (0.2 M), potential scanning rate 100 mV/s.

potentials, for a two-layer film it is broader, and for a three-layer film it is shifted to higher potentials. Among 1-3-layer films, the largest ECL signal is usually observed for a two-layer film. Eight-layer films give a peak that is shifted by +200 mV relative to single-layer films, with a narrow symmetrical shape. These results confirm that film thickness and structure affect electrochemical processes and the shape of the ECL signal, consistent with the literature data [20]. As shown in the first studies of ECL in LB films [27], the accessibility and efficiency of phosphor excitation depends on the orientation of the molecule in the film and its structure, so the shape of the ECL curve may depend on the type and thickness of the film.

3.6 Application of modified electrodes for ECL analysis

Fig. 12 shows the dependence of the peak ECL intensity for PMMA/DPA films of different types (1-layer Z-type, 2-layer Y-type, 3-layer YX-type) on the concentration of the coreactant Ph_4BNa. As can be seen from the figure, the sensitivity of the films as sensors increases with the number of layers. The negative logarithms of the concentration values and the maximum light intensity were used for calibration. Table 5 shows corresponding calibration equations

In general, the confidence interval of the angular coefficient values for the three types of films is almost the same, which indicates statistically insignificant differences between them. However, the graphs show that an increase in the number of film layers leads to an increase in the intensity of the ECL signal, which is especially important at low concentrations and is manifested in a change of the free term in the graduation dependence. Several conclusions can be drawn from this result. Firstly, the relationship between light intensity and concentration in logarithmic units is linear, which is confirmed by the high coefficient of determination. Secondly, an increase in the number of film layers leads to an increase in the sensitivity of the system (lower limit of detection), since although the angular coefficient remains almost unchanged, the free term of the equation changes significantly, indicating an increase in the intensity of the ECL signal.

4. Conclusions

In this work, the formation conditions, morphology, optical and electrochemical properties of Langmuir-Blodgett films with phosphors of the polycyclic aromatic hydrocarbons class and their potential use as sensors for ECL analysis are investigated.

Changes in the wetting angle for different types of films indicate that hydrophilicity and hydrophobicity depend on the film structure and the number of its layers. The results of the study are in line with theoretical expectations, showing that the wettability of monomeric films changes less pronouncedly than that of polymeric films. The solid-phase fluorescence method showed that PMMA is a more efficient medium for phosphor immobilisation compared to the HSt monomer. The study of surface morphology indicates a slow degradation of the electrodes during electrolysis. The application of the films changes the surface topology, in particular, the surface becomes more granular on degraded electrodes, and homogeneous on new ones. Y-type films exhibit high thermodynamic stability and effectively isolate oxide grains, reducing electrode degradation and leaving the surface more inert but permeable to reactions. An increase in the number of film layers leads to passivation of the electrode surface, which reduces the availability of electrons for redox processes and degrades the sensitivity of the sensor, especially at low analyte concentrations. ECL studies have shown that the film thickness significantly affects the intensity and shape of the ECL signal, with bilayer films showing the strongest signal. The obtained linear relationship between the ECL intensity and the concentration of the coreactant indicates the prospects of using such types of modified electrodes as a platform for the development of analytical ECL systems.

The work was supported by the projects of the Ministry of Education and Science of Ukraine No. 0124U000601 and No. 0122U001533 and the National Research Foundation of Ukraine (registration number 2020.02/0390).

5. References

1. W. Miao, *Chem. Rev.*, **108,** 2506, 2008, doi: 10.1021/cr068083a.
2. G. F. Blackburn *et al.*, *Clin. Chem.*, **37**, 1534, 1991. doi: 10.1093/clinchem/37.9.1534.
3. L. Bouffier and N. Sojic, ‘Chapter 1. Introduction and Overview of Electrogenerated Chemiluminescence’, in *Detection Science*, N. Sojic, Ed., Cambridge: Royal Society of Chemistry, 2019, pp. 1–28. doi: 10.1039/9781788015776-00001.
4. A. J. Bard, Ed., *Electrogenerated Chemiluminescence*, CRC Press, 2004. doi: 10.1201/9780203027011.
5. S. Mahadevarao Premnath and M. Zubair, ‘Electrochemiluminescence Method’, in *StatPearls*, Treasure Island (FL): StatPearls Publishing, 2024. http://www.ncbi.nlm.nih.gov/books/NBK594228/ (accessed 08 November 2024).
6. E. Scorsone, S. Stewart, and M. Hamel, *Sensors*, vol. 24, no. 11, p. 3627, 2024, doi: 10.3390/s24113627.
7. J. Wu and H. X. Ju, ‘Clinical Immunoassays and Immunosensing’, in *Comprehensive Sampling and Sample Preparation*, Elsevier, 2012, pp. 143–167. doi: 10.1016/B978-0-12-381373-2.00071-5.
8. R. Wilson, C. Clavering, and A. Hutchinson, *Anal. Chem.*, **75**, 16, 4244, 2003, doi: 10.1021/ac034163s.
9. H. S. White and A. J. Bard, *J. Am. Chem. Soc.*, **104**, 6891, 1982, doi: 10.1021/ja00389a001.
10. Z. Liu, W. Qi, and G. Xu,, *Chem. Soc. Rev.*, 44, 3117, 2015, doi: 10.1039/C5CS00086F.
11. K. Brown, R. S. Blake, D. W. Robinson, and L. Dennany, *J. Electroanal. Chem.*, **941**, 117521, 2023, doi: 10.1016/j.jelechem.2023.117521.
12. W. Miao and J.-P. Choi, ‘Chapter 5. Coreactants’, in *Electrogenerated chemiluminescence*, A. J. Bard, Ed., New York: M. Dekker, 2004, pp. 224–283 . doi: 10.1201/9780203027011-7.
13. A. J. Bard, J. D. Debad, J. K. Leland, G. B. Sigal, J. L. Wilbur, and J. N. Wohlstadter, ‘Chemiluminescence, Electrogenerated’, in *Encyclopedia of Analytical Chemistry*, 1st ed., R. A. Meyers, Ed., Wiley, 2000. doi: 10.1002/9780470027318.a5302.
14. H. Ahsan, *Comp. Clin. Pathol.*, **31**, 333, 2021, doi: 10.1007/s00580-021-03302-4.
15. L. Bouffier, S. Arbault, A. Kuhn, and N. Sojic, *Innov. Technol.*, May 2018, doi: 10.51257/a-v1-p156.
16. X. Lv *et al.*, *Appl. Bio Mater.*, **3**, 8933, 2020, doi: 10.1021/acsabm.0c01201.
17. J.-L. Liu, Z.-L. Tang, J.-Q. Zhang, Y.-Q. Chai, Y. Zhuo, and R. Yuan, *Anal. Chem.*, **90**, 5298, 2018, doi: 10.1021/acs.analchem.8b00209.
18. V. Gaudin, ‘Receptor-based electrochemical biosensors for the detection of contaminants in food products’, in *Electrochemical Biosensors*, Elsevier, 2019, pp. 307–365. doi: 10.1016/B978-0-12-816491-4.00011-5.
19. M. Dramićanin, ‘Lanthanide and Transition Metal Ion Doped Materials for Luminescence Temperature Sensing’, in *Luminescence Thermometry*, Elsevier, 2018, pp. 113–157. doi: 10.1016/B978-0-08-102029-6.00006-3.
20. Y. Zholudov, D. Snizhko, A. Kukoba, H. Bilash, and M. Rozhitskii, *Electrochimica Acta*, **54**, 360, 2008, doi: 10.1016/j.electacta.2008.07.069.
21. A. Fujimori, ‘Langmuir-Blodgett (LB) Film’, in *Encyclopedia of Polymeric Nanomaterials*, S. Kobayashi and K. Müllen, Eds., Berlin, Heidelberg: Springer Berlin Heidelberg, 2014, pp. 1–7. doi: 10.1007/978-3-642-36199-9_145-1.
22. Y. Zholudov, D. Snizhko, A. Kukoba, and O. Bilash, ‘Automated Electrochemiluminescent Analyzer for Research and Biomedical Assay’, in *2021 IEEE 8th International Conference on Problems of Infocommunications, Science and Technology (PIC S&T)*, Kharkiv, Ukraine: IEEE, Oct. 2021, pp. 439–444. doi: 10.1109/PICST54195.2021.9772152.
23. D. Snizhko, A. Bykh, B. Lou, and G. Xu, *Przegląd Elektrotechniczny*, **7**, 29, 2021, doi: 10.15199/48.2021.07.0.
24. O. N. Bezkrovnaya, Y. N. Savin, and M. V. Dobrotvorskaya, *Functional Materials*, *13*, 687, 2006.
25. D. Martynov, D. Snizhko, M. Slipchenko, and Y. Zholudov, ‘Technology of Electrochemiluminescence Sensors Based on Langmuir-Blodgett

Films with Polycyclic Organic Phosphors', in *2023 IEEE 4th KhPI Week on Advanced Technology (KhPIWeek)*, Kharkiv, Ukraine: IEEE, Oct. 2023, pp. 1–5. doi: 10.1109/KhPIWeek61412.2023.10312840.

26. D. Martynov, Y. Zholudov, and D. Snizhko, UA patent #152984, 2023.
27. Y. S. Obeng and A. J. Bard, *Langmuir*, **7**, 195, 1991, doi: 10.1021/la00049a035.
28. P. Dynarowicz-Latka, A. Wnętrzak, and A. Chachaj-Brekiesz, *J. R. Soc. Interface*, **21**, 20230559, 2024, doi: 10.1098/rsif.2023.0559.
29. H. Seo *et al.*, *Adv. Mater.*, **29**, 1605587, 2017, doi: 10.1002/adma.201605587.
30. Y. Zholudov, O. Bilash, A. Kukoba, M. Rozhitskii, *The Analyst*, **136**, 598, 2011, doi: 10.1039/C0AN00589D.